$$\Delta m_{c,g} = m_c (x_c - x_0) \tag{15}$$

If we consider the evaporator section to be a closed system, pressure and vapor mass in this section increases when temperature increases. In contrast, pressure and vapor mass in the condenser section decreases when temperature decreases. But in fact, the evaporator and condenser sections are connected together. Thus, while there is a change of temperature, the vapor mass in the evaporator will expand and the vapor mass in the condenser will collapse, the pressure inside will be kept constant at an arbitrary value along the entire CLOHP. Thus, the expansion and collapse results from a change of vapor mass and the net change of vapor mass is equivalent to the net vapor volume expansion/collapse. From the above discussion, we can set an equation for a suitable startup condition as follows:

$$\Delta m_{c,g} - \Delta m_{e,g} > 0 \tag{16}$$

Calculating the temperature for a suitable startup condition can be done by setting the temperature of the high temperature reservoir. Next, determine the highest temperature for the low temperature reservoir from which a suitable startup condition can be achieved. This temperature can be found by setting

$$\Delta m_{c,g} = \Delta m_{e,g} \tag{17}$$

The method of trial and error was selected to find the solution. The calculation flow chart is as shown in figure 8.

Comparison of results from the mathematical model with the experimental data

The experiment in this paper was conducted by increasing heat input step by step and observing whether the CLOHP could start to transfer heat or not. In the case of a start up failure, the experiment was continued by increasing the temperature of the evaporator section. This could be done because the evaporating temperature at the beginning of the experiment was low therefore, dry spot did not occur. The calculation in this case was done by setting the temperature at initial state equal to the evaporator temperature of previous start up failures. This could be done because the heat is uniformly distributed along the CLOHP when a state of startup failure occurs.

The comparison of the results from the mathematical model with the experimental data, in which R123 was used as the working fluid, is shown in figure 9. The horizontal axis shows the calculated value of the minimum temperature difference, between the evaporator and condenser section, which produces a successful start up. The vertical axis shows the temperature difference measured from the experiment. In practice, it is difficult to control the state for an exact suitable startup. Therefore, the received data consists of temperature differences, between the evaporator and condenser sections for both successful and unsuccessful start ups. Figure 9 shows all of the data divided in to two zones as follows:

- The upper zone shows the temperature differences for suitable startup conditions where the CLOHP was in a successful startup state. The temperature differences measured from the data from the experiments shown in this zone were higher than the value calculated from the model.
- The lower zone shows the temperature differences for unsuitable startup conditions and the start ups failed. The temperature differences measured from the data from the experiments in this zone were lower than the values calculated from the model.

In addition, all the CLOHP's start ups (successful or failed) which were detected from the experiment are also shown. The rectangular mark shows a successful start up and the circular mark shows a failed start up.

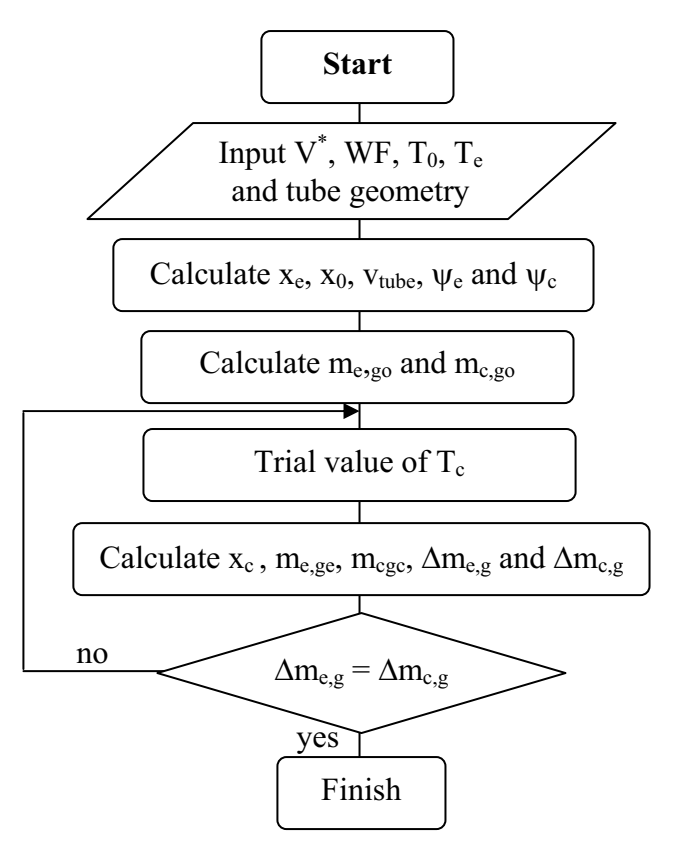


Figure 8 the suitable startup condition calculation flow chart

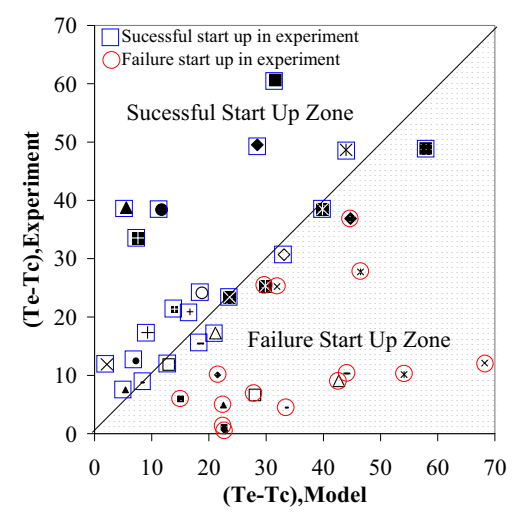


Figure 9a. the result from modeling compared with experimental data

Symbol	Le	Di	N	angle
•	100	0.66	5	90
•	100	0.66	10	90
•	100	0.66	15	90
×	50	1.06	5	90
×	100	1.06	5	90
•	150	1.06	5	90
+	50	1.06	10	90
-	100	1.06	10	90
-	150	1.06	10	90
\Diamond	50	1.06	15	90
	100	1.06	15	90
Δ	150	1.06	15	90
\times	50	1.5	5	90
Ж	100	1.5	10	90
0	150	1.5	15	90
#	50	2.03	5	90
•	100	2.03	5	90
	150	2.03	5	90
A	50	2.03	10	90
×	100	2.03	10	90
Ж	150	2.03	10	90
•	50	2.03	15	90
+	100	2.03	15	90
	150	2.03	15	90

Figure 9b. symbol interpretation table

Figure 9 shows that this model can efficiently predict the temperature for suitable startup conditions. There were only 6 pieces of data showing missed predictions. In the experiment, they were successful, but the model predicted that they would fail. However, the data was shown to fall very closely to the boundary between both zones. Thus, it can be said that this model has good accuracy. When the 6 pieces of data are compared with the measured value from the experiment, this model gives 16% accuracy. However, more experiments are needed to confirm this.

This model shows that when the inside diameter follows Maezawa criteria and the evaporator and condenser lengths are equal, the tube geometry does not have an effect on the temperature difference for a suitable successful start up. Moreover, an unsuitable temperature difference produces the net vapor expansion to be more than the net vapor collapse and the replacement process is obstructed. The CLOHP, consequently, fails to start up. Thus, it is not enough to attribute a suitable startup condition to only a super heated level at the evaporator section. The control of suitable temperature differences between the evaporator and condenser sections is the most important.

In addition, this model indicates that the filling ratio also has an effect on the temperature difference for a suitable startup condition. Figure 10 shows a simulation of the effect of the filling ratio on the temperature difference for a suitable startup condition (T_e-T_c) . In this case the evaporator temperature was controlled at 45 degrees Celsius. The figure shows that the value of T_e-T_c is high at a small filling ratio while the value of T_e-T_c decreases rapidly at a filling ratio of more than 0.5. This trend indicates that it is very difficult to have a successful startup with a small filling ratio. It is because a large temperature difference is needed. For a large filling ratio, a small temperature difference is required for a successful startup. It is, thus, easier to start up. This result agrees with Lin et al. (2000). They reported that their oscillating heat pipe could not operate at a filling ratio of less than 32% although only a heat input of 200 watts was applied.

It can be concluded that the filling ratio strongly affects the temperature difference for a suitable startup condition. In the case of a fixed evaporator temperature and a small filling ratio, a large temperature difference is needed in order to have a successful start up; vice versa for a large filling ratio.

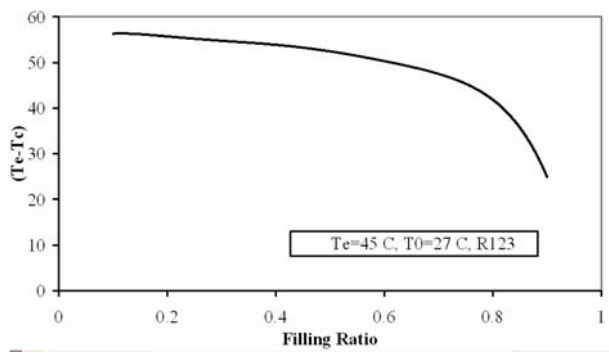


Figure 10 the effect of filling ratio on the temperature difference required for successful start up

CONCLUSION

This paper presents the consideration for a suitable startup condition for a CLOHP using both a visual study and quantitative experiments. It was found that a CLOHP is able to have a successful start up when the replacement process occurs inside. It can be achieved when more net vapor collapses than expands. Obstruction of the replacement process results when less vapor collapses than expands. This obstruction leads to startup failure and initial dryout if high temperature is applied to the CLOHP. In addition, this paper conducted a mathematical model to predict the temperature for a suitable startup. The comparison of results from the model and experiment was also conducted. The model gave a good prediction with a 16% accuracy. This model also indicated that:

- 1. The temperature difference between the evaporator and condenser sections is an important parameter for suitable startup conditions.
- 2. The filling ratio strongly affects the temperature difference for a suitable startup condition. In the case of a fixed evaporator temperature and a small filling ratio, a large temperature difference is needed in order to have a successful startup state and vice versa for large filling ratios.

NOMENCLATURE

working fluid mass, kg

M

	5 p = 0.000 p
V	volume, m ³
V^*	filling ratio
V	specific volume, m ³ /kg
X_c	thermodynamics vapor quality inside the condenser in a low temperature
	reservoir
X_e	thermodynamics vapor quality inside the evaporator in a high temperature
	reservoir
X_{O}	thermodynamics vapor quality at initial state
$\Delta m_{c,g}$	decrease mass in condenser section due to change in temperature from an
	initial to a low temperature
$\Delta m_{e,g}$	decrease mass in evaporator section due to change in temperature from an
	initial to a high temperature
ρ	working fluid density, kg/m ³
Ψc	ratio of condenser's volume by CLOHP's volume
Ψe	ratio of evaporator's volume by CLOHP's volume
1 *	1

Subscripts

c	property of working fluid in the condenser section
c, gc	property of vapor phase in the condenser section in a low
	temperature reservior
c, go	property of vapor phase in the condenser section at initial state
condenser	condenser section
e	property of working fluid in the evaporator section
e, ge	property of vapor phase in the evaporator section in a high
	temperature reservior
e, go	property of vapor phase in the evaporator section at initial state
evaporator	evaporator section
f	liquid phase
f,c	liquid phase in a low temperature reservoir
f,e	liquid phase in a high temperature reservoir
fg	different value between property of vapor and liquid phase
fg,c	different value between property of vapor and liquid phase inside
	condenser in a low temperature reservoir
fg,e	different value between property of vapor and liquid phase inside
	evaporator in a high temperature reservoir
fill	property of working fluid at filling state
g	vapor phase
0	initial state
tube	container of CLOHP

Acknowledgements

All of this work could not have been conducted without the support from the Thailand Research Fund (contract no.BRG4780024) The authors would also like to express their sincere appreciation.

REFERENCES

- [1] Charoensawan, P., Khandekar, S., Groll, M., and Terdtoon, P., Closed Loop Pulsating Heat Pipe Part A: Parametric Experimental Investigations. *Applied Thermal Engineering*. Vol. 23., 2003.
- [2] Charoensawan, P., Terdtoon, P., Tantakom, P., and Ingsuwan, P., Effect of Evaporator Section Lengths, Number of Turns and Working Fluid on Internal Flow Patterns of a Vertical Closed-Loop Oscillating Heat Pipe. *Procs. of the 7th International Heat Pipe Symposium.* Jeju Korea., 2003.
- [3] GI, K., Sato, F., and Maezawa, S., Flow Visualization Experiment on Oscillating Heat Pipe. *Procs. of the 11th International Heat Pipe Conference*, Tokyo Japan., 1999.
- [4] Khandekar, S., Charoensawan, P., Groll, M., and Terdtoon, P., Closed Loop Pulsating Heat Pipe Part B: Visualization and Semi-Empirical Modeling. *Applied Thermal Engineering*. Vol. 23., 2003.
- [5] Kammuang-lue, N., Charoensawan, P., Ritthidech, S., Budhajan, K. and Terdtoon, P., Effect of Working Fluids on Heat Transfer Characteristics of A Closed-Loop Pulsating Heat Pipe at Critical State. *Proceedings of the 1st International Seminar on Heat Pipes and Heat Recovery Systems*. Kuala Lumpur Malaysia., 2004

- [6] Lee, W., Jung, H., Kim, J., and Soo Kim, J., Characteristics of Pressure Oscillation in Self-excited Oscillating Heat Pipe based on Experimental Study. *Procs. of the 6th International Heat Pipe Symposium*. Chiang Mai Thailand., 2000.
- [7] Lin, L., Ponnappan, R. and Leland, J., Experimental Investigation of Oscillating Heat Pipe. 35th Energy Conversion Engineering Conference and Exhibit. Vol. 2., 2000.
- [8] Maesawa, S., Gi, K.Y., Minamisawa, A., and Akachi, H., Thermal Performance of Capillary Tube Thermosyphon. *Procs. of the IX International Heat Pipe Conference*. Albuquerque USA. Vol. II., 1996.
- [9] Maesawa, S., Heat Pipe: Its Origin, Development and Present Situation. *Procs. of the* 6th *International Heat Pipe Symposium*. Chiang Mai Thailand., 2000.
- [10] Qu, W., and Ma, T., Experimental Investigation on Flow and Heat Transfer of a Pulsating Heat Pipe. *Procs. of the 12th International Heat Pipe Conference*. Russia., 2001.
- [11] Qu, W., and Ma, H.B., Theoretical analysis of startup of a pulsating heat pipe. *International Journal of Heat and Mass Transfer* (ARTICLE IN PRESS)
- [12] Soponpongpipat, N., Sakulchangsatjatai, P., Saiseub, M. and Terdtoon, P., Time Response Model of Operational Mode of Closed-Loop Oscillating Heat Pipe at Normal Operating Condition., *Procs. of the 8th International Heat Pipe Symposium. Kumamoto* Japan., 2006.
- [13] Wong, T.N., Tong, B.Y., Lim, S.M., and Oci, K.T., Theoretical Modeling of Pulsating Heat Pipe. *Procs. of the 11th International Heat Pipe Conference*. Musashinoshi Tokyo Japan., 1999.

Biographies

Nitipong Soponpongpipat received his Masters degree in Mechanical Engineering from Chiang Mai University, Thailand in 2000. At present he is a Ph.D student in the Department of Mechanical Engineering at Chiang Mai University and a member of staff in the Department of



Mechanical Engineering at Silpakorn University, studying heat transfer behavior of Closed Loop Oscillating Heat Pipes at normal operation.

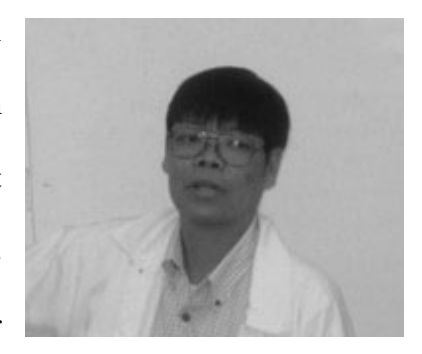
Phrut Sakulchangsatjaati received his Ph.D in Mechanical Engineering from Chiang Mai University, Thailand in 2006. At present he is a member of staff in the Department of Mechanical Engineering at Chiang Mai University. His main interests have been simulation models in pulsating heat pipes.



Niti Kammuang-lue received his Bachelor degree in Mechanical Engineering from Chiang Mai University, Thailand in 2002. At present he is a Ph.D student in the Department of Mechanical Engineering at Chiang Mai University, studying maximum heat transfer capacity of Closed Loop Oscillating Heat Pipes.



Pradit Terdtoon is currently a Professor of Mechanical Engineering, and Director of the Heat Pipe and System Laboratory in the Department of Mechanical Engineering at Chiang Mai University, Thailand. Current research areas include the theory and application of a heat pipe, heat transfer



application of heat pipe technology for waste heat recovery and simulation of blood flow.

ภาคผนวก ค

บทความ

Prediction Model of Average Heat Transfer Capacity of Closed-Loop Oscillating Heat Pipe at Normal Operating Condition

Prediction Model of Average Heat Transfer Capacity of Closed-Loop Oscillating Heat Pipe at Normal Operating Condition

N. Soponpongpipat, P. Sakulchangsatjatai, S. Promdan and P. Terdtoon Department of Mechanical Engineering, Faculty of Engineering, Chiang Mai University, Thailand 50200. Tel. +66-53-944151 Fax. +66-53-226014 Email: Nitipongsopon@hotmail.com

Abstract

Although the heat transfer characteristic of CLOHP varies with time, in engineering application, its average heat capacity is much preferable. This research, thus, makes an attempt to establish the mathematical model for predicting the average heat transfer rates of CLOHP at normal operating condition by using the concept of "average" thermal resistance that occurred at any position of CLOHP. In this research, five thermal resistances are presumed to exist in CLOHP. The first and second are thermal resistances between the heat source and evaporator external surface and thermal resistances between the condenser external surface and heat sink. The third and fourth are thermal resistances across the thickness of the container wall in the evaporator and the condenser. The others, internal thermal resistance, are thermal resistance of convection and boiling fluid inside CLOHP in the evaporator and thermal resistance of convection and condensing fluid in the condenser. Modeling of the internal thermal resistance is the target of this research. The modeling can be done by enhancing the concept that the internal thermal resistances are resulted from the superposition between convection and boiling of working fluid inside. In addition, the phase change damping coefficient (PCDC), the parameter which to be used to describe the heat transfer characteristic of CLOHP, is introduced in this paper. The precision of model is examined by using the experimental data of R123 CLOHP at bottom heat mode. It is found that the model give 19.60% accuracy. Finally, the characteristic of CLOHP is also described by means of PCDC.

Key Words: CLOHP, Model, PCDC

1. INTRODUCTION

The Closed Loop Oscillating Heat Pipe (CLOHP) is a one type of heat exchanger. It is constructed by meander the capillary tube and connects its both ends together to form the loop of bundle tube [5]. Heat is transferred by oscillation of working fluid inside the CLOHP.

It was known that the heat transfer characteristic of CLOHP varies with time. There were many previous studies, thus, model the time depending heat transfer rates of CLOHP. Dobson and Harms [3] conducted the Lumped Parameter Model which was the simple model that explained the oscillating behavior of working fluid inside CLOHP. This model was developed later by Swanepoel et al [7]. Wong [8] established the theoretical model to determine the local heat input pass through vapor slug. All of above model give the basic concept of CLOHP operation and confirm its oscillating behavior. However, it can't predict the actual heat transfer rates. The attempt to develop the heat transfer rates model was done by Shaffi et al. [6]. They conducted the model for CLOHP and CEOHP (Closed End Oscillating Heat Pipe). This model can predict the heat transfer rate of working fluids at any time and position of OHP. The calculation, however, seem complex and inconvenience to use in practical. Moreover, the average heat transfer rates are more preferred in engineering application. The model of average thermal resistance occurred at any position of CLOHP give a more simplicity and good understanding. This concept was presented in heat transfer rates calculation of heat pipe and thermosyphon [ESDU 81038]. Dobson et al. [4] adapted this concept with CLOHP. Although their work gives a good agreement with experimental data, this model couldn't give the detail of occurring heat transfer resistance inside CLOHP. Thus, the explanation of the effect of CLOHP geometry on heat transfer rates is difficult to do. In this paper, the heat transfer mechanism inside CLOHP will be discussed. The result from discussion will lead to the modeling of internal thermal resistance. Finally this paper shows the incomplete condensation situation which is a specific character and effect on the CLOHP's heat transfer rates. This situation can be taken into account to model by the term Phase Change Damping Coefficient (PCDC).

2. METHOD OF MODELING

2.1 Thermal resistance of CLOHP

As shown in figure 1, there are 9 thermal resistances on CLOHP. They consist of

- Thermal resistance due to heat convection of heating medium at evaporator section (Z_1)
- Thermal resistance due to radius heat conduction through the wall of capillary tube at the evaporator section (Z_2)
- Thermal resistance due to heat convection of working fluid inside tube at evaporator section (Z_3)

- Thermal resistance due to convection boiling of working fluid at evaporator section (Z_4)
- Thermal resistance due to condensation of working fluid at condenser section (Z_5)
- Thermal resistance due to heat convection of working fluid inside tube at condenser section (Z_6)
- Thermal resistance due to radius heat conduction through the wall of capillary tube at the condenser section (\mathbb{Z}_7)
- Thermal resistance due to heat convection of cooling medium at condenser section (Z_8)
- Thermal resistance due to longitudinal heat conduction from evaporator to condenser section (Z_9)

The total thermal resistance can be written as follows,

$$Z_{total} = Z_{1} + \left[\left(Z_{2} + \left(Z_{3}^{-1} + Z_{4}^{-1} \right)^{-1} + \left(Z_{5}^{-1} + Z_{6}^{-1} \right)^{-1} + Z_{7} \right)^{-1} + \left(Z_{9} \right)^{-1} \right]^{-1} + Z_{8}$$

$$(1)$$

If the Z_9 thermal resistance have a large order comparing with the other thermal resistance, equation (1) will be reduced to

$$Z_{total} = Z_{1} + Z_{2} + \left(Z_{3}^{-1} + Z_{4}^{-1}\right)^{-1} + \left(Z_{5}^{-1} + Z_{6}^{-1}\right)^{-1} + Z_{7} + Z_{8}$$
(2)

Generally, order of magnitude of Z_1 and Z_8 thermal resistance are larger than the others. They can be determined from well known equation. Thus to avoid misleading of modeling due to order of magnitude of Z_1 and Z_8 thermal resistance, they will not be taken into account to model. This research will consider the other thermal resistance and equation (2) can be written by

$$Z_{total} = Z_{2} + \left(Z_{3}^{-1} + Z_{4}^{-1}\right)^{-1} + \left(Z_{5}^{-1} + Z_{6}^{-1}\right)^{-1} + Z_{7}$$
(3)

The average heat transfer rates of CLOHP can be calculated from equation (4)

$$Q = \frac{\Delta T_s}{Z_{total}}$$
 (4)

 ΔT_s represent the temperature different between outside surface of evaporator and condenser section.

2.2 The Z_2 and Z_7 thermal resistance

The thermal resistance due to radius heat conduction through the wall of capillary tube at the evaporator section (Z_2) and the thermal resistance due to radius heat conduction through the wall of capillary tube at the condenser section (Z_7) can be determined from equation (5) and (6)

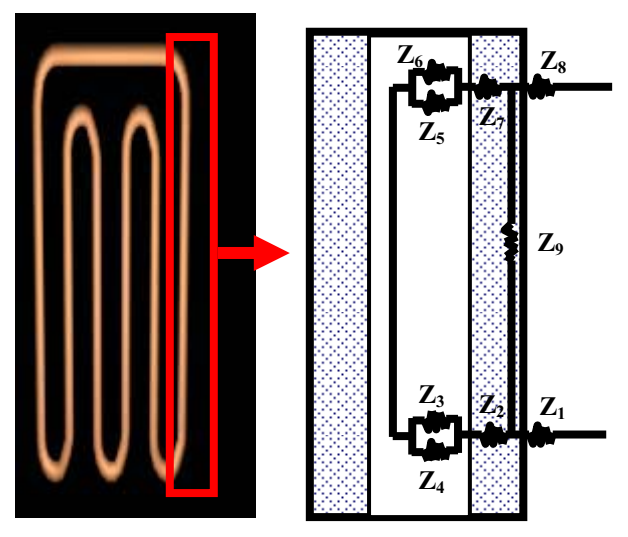


Fig.1 Thermal resistance of CLOHP

$$Z_{2} = \frac{\ln(D_{O}/D_{i})}{2\pi k_{e}(2nL_{e})}$$
 (5)

$$Z_{\tau} = \frac{\ln(D_O / D_i)}{2\pi k_c (2nL_c)} \tag{6}$$

 D_{o} and D_{i} means the outside and inside diameter of tube respectively. k_{e} and k_{c} are the thermal conductivity of material at evaporator and condenser section. L_{e} and L_{c} represent the length of evaporator and condenser section.

2.3 The Z_3 and Z_6 thermal resistance

In order to clarify the concept of Z_3 and Z_6 thermal resistance modeling, we will consider the flow pattern inside CLOHP as shown in figure 2. This figure is visualization data taken from Plexiglas CLOHP. The experiment was done by heating the evaporator at bottom side of figure and cooling the condenser at the top side of figure. Electric heater was used as heat source. Heat passed to CLOHP by conduction through the high conductivity silicone paste. The silicone was pasted between heater and CLOHP. Water was use as cooling medium. The evaporator, adiabatic and condenser length is 50 mm. The working temperature is maintained at 220°C. The visual study data were taken by highresolution charge-coupled device (CCD) still camera of speed 30 images per second with one million pixels resolution. The flow pattern inside CLOHP will be observed continuously until experiment is over.

By marking the vapor slug with a black circle, we can see from the figure 2 that the vapor slug moves forward to evaporator section which locate at the bottom of figure. The liquid below the marked vapor slug will also move to evaporator section. The more distance liquid passes through evaporator section, the more violent in boiling. From this phenomenon, we can make assumption that the

heat transfer mechanisms between inside wall tube and working fluid are superposition of single phase convection heat transfer and free convection boiling heat transfer of working fluid.

We will, beforehand, consider a single phase convection heat transfer. The free convection boiling heat transfer will, eventually, be determined.

The single phase convection heat transfer of working fluid inside CLOHP can be determined from Gnielinski's equation.

om Gnielinski's equation.

$$Nu_{e} = \frac{\left(\frac{f}{8}\right)(Re_{e} - 1000)Pr_{e}}{1 + 1.27\left(\frac{f}{8}\right)^{\frac{1}{2}}\left(Pr_{e}^{\frac{2}{3}} - 1\right)}$$

$$-1 + 1.27\left(\frac{f}{8}\right)^{\frac{1}{2}}\left(Pr_{e}^{\frac{2}{3}} - 1\right)$$

$$-1 + 1.27\left(\frac{f}{8}\right)^{\frac{1}{2}}\left(P$$

Fig.2 shown the flow pattern inside CLOHP

Nu_e is the Nusselt Number and Pr_e is Prandtl Number in evaporator section. f is the friction coefficient determined from equation (8)

$$f_e = (0.79 \ln Re_e - 1.64)^{-2}$$
 (8)

. At 1/10 second after beginning

Re show the Reynolds Number at evaporator section which is determined from equation (9)

$$Re_e = \frac{\rho_{mix} u_e D_\iota}{\mu_{mix}} \tag{9}$$

Mixture density (ρ_{mix} = 1/ v_{mix}) and mixture velocity (μ_{mix}) determined from equation (10)

$$\Omega_{\text{mix}} = \Omega_{\text{f}} + x\Omega_{\text{fg}} \tag{10}$$

A property of working fluid used in calculation is the values corresponding to the working temperature (T_{ν}) of CLOHP.

$$T_V = T_{Se} + \left[Z_2 + (Z_3^{-1} + Z_4^{-1})^{-1}\right] \frac{\Delta T_S}{Z_{total}}$$
 (11)

Tv and Ts shown the working temperature and outside evaporator surface temperature of CLOHP respectively.

The average quality of mixture can be calculated from equation (12)

$$x = \frac{\left(\frac{1}{\rho_0 V^*} - \frac{1}{\rho_f}\right)}{\left(\frac{1}{\rho_v} - \frac{1}{\rho_f}\right)}$$
(12)

 ρ_0 is liquid density of working fluid at filling temperature. V^+ is the filling ratio, the ratio of liquid filling volume by total volume of CLOHP.

The velocity of working fluid in evaporator section will be found from heat balance equation (13)

$$Q_{e} = \rho_{\text{mix},T_{v}} \left(\frac{\pi D_{i}^{2}}{4} \right) v_{e} \left(h_{eo} - h_{ei} \right)$$
 (13)

$$h_{eo} = h_{eo,f} + xh_{eo,fg}$$
; Pr operty at $T_{se,i}$ (14)

$$h_{ei} = c_c T_{sc}$$
; Property at $T_{sc,i}$ (15)

 $T_{se,i}$ and $T_{sc,i}$ are inside surface temperature of evaporator and condenser respectively. h_{eo} and h_{ei} are enthalpy of working fluid at exit and entrance of evaporator.

According to the relation between Nusselt Number and convection heat transfer coefficient, Equation (7) can be rewritten in form of thermal resistance due to convection of working fluid as follow.

$$Z_3 = \frac{D_i}{k_{\text{mix},Tv} Nu_e \left[2\pi r_i \left(2nL_e \right) \right]}$$
 (16)

By using the same concept as describe above, we can find Z_5 thermal resistance from

$$Z_{6} = \frac{D_{i}}{k_{mix,Tv} Nu_{c} \left[2\pi r_{i} \left(2nL_{c} \right) \right]}$$
(17)

 $k_{mix,Tv}$ is the thermal conductivity of working fluid mixture at working temperature.

2.4 The Z₄ and Z₅ thermal resistance

The free convection boiling heat transfer coefficient can be calculated from Foster and Zuber equation,

$$h_b = 0.00122 \left[\frac{k_l^{0.79} c_{pl}^{0.45} \rho_l^{0.49}}{\sigma^{0.5} \mu_l^{0.29} (\rho_g h_{fg})^{0.24}} \right] \Delta T^{0.24} \Delta P^{0.75}$$
 (18)

Associating with the Claperyron Equation,

$$\left(\frac{\mathrm{dP}}{\mathrm{dT}}\right)_{\mathrm{sat}} = \frac{\mathrm{h}_{\mathrm{fg}}}{\mathrm{T}(\mathrm{v}_{\mathrm{g}} - \mathrm{v}_{\mathrm{l}})} \tag{19}$$

Equation (18) will be rewritten into

$$h'_{b} = \sqrt{0.00122} \left[\frac{k_{l}^{0.79} c_{pl}^{0.45} \rho_{l}^{0.49}}{\sigma^{0.5} \mu_{l}^{0.29} (\rho_{g} h_{fg})^{0.24}} \right] \left(\frac{Q}{2n\pi DL} \right) \left[\frac{h_{fg}}{(v_{g} - v_{l}) T_{sat.wall}} \right]^{0.75}$$

$$(20)$$

Equation (20) can be written in form of thermal resistance as follow

$$z_{b} = \frac{1}{\sqrt{0.00122 \left[\frac{k_{l}^{0.79} c_{pl}^{0.49} \rho_{l}^{0.49}}{\sigma^{0.5} \mu_{l}^{0.29} (\rho_{g} h_{fg})^{0.24}}\right]} (2Qn\pi DL) \left[\frac{h_{fg}}{(v_{g} - v_{l})T_{sat.evapwall}}\right]^{0.75}}$$
(21)

Thus, the Z₄ thermal resistance can be determined from

$$Z_{4} = \frac{1}{\sqrt{0.00122 \left[\frac{k_{l}^{0.79}c_{pl}^{0.45}\rho_{l}^{0.49}}{\sigma^{0.5}\mu_{l}^{0.26}(\rho_{g}h_{f_{g}})^{0.24}}\right]} (2Qn\pi D_{l}L_{e}) \left[\frac{h_{fg}}{(v_{g}-v_{l})T_{sat.evap\ wall}}\right]^{0.75}}$$
(22)

By approximation that condensation is a reverse process of evaporation. The Z_5 thermal resistance, thus, can be determined from

$$Z_{s} = \frac{1}{\sqrt{0.00122 \left[\frac{k_{l}^{0.79} c_{pl}^{0.45} \rho_{l}^{0.49}}{\sigma^{0.5} \mu_{l}^{0.29} (\rho_{g} h_{fg})^{0.24}}\right] (2Qn\pi D_{i} L_{c}) \left[\frac{h_{fg}}{(v_{g} - v_{l}) T_{sat.con\ wall}}\right]^{0.75}}}$$

$$(23)$$

2.5 The Phase Change Damping Coefficient (PCDC)

Consider the flow pattern of working fluid inside CLOHP as shown in figure 3, we can see that working fluid in form of mixture is in both condenser and evaporator section. This situation shows the incomplete condensation, otherwise liquid will occupy all condenser volume. Incomplete condensation results in decreasing of condensing liquid. When the condensing liquid decrease, transferred heat carried by evaporation of liquid in next step will also decrease. In addition, volume of vapor remaining in condenser section due to incomplete condensation is cause of decreasing in working fluid velocity. Heat transfer rated of CLOHP, consequently, decrease.

For situation above, the incomplete condensation results in under estimation of values calculated from equation (16), (17), (22), (23) and average heat transfer rates are overestimated. Thus, the effect of incomplete condensation will be taken into account by introduced the PCDC. By using the PCDC, equation (3) can be rewritten into equation (24)

$$Z_{total} = Z_{2} + S_{e} \left(Z_{3}^{-1} + Z_{4}^{-1} \right)^{-1} + S_{c} \left(Z_{5}^{-1} + Z_{6}^{-1} \right)^{-1} + Z_{7}$$
 (24)

Determination of PCDC values can be done by using experimental data of which the experiment has been conducted by setting evaporator and condenser to by symmetry. We can accordingly expect that PCDC are equal both in evaporator and condenser section. The PCDC correlation, consequently, can be basically found. This research employes experimental data of Khummuang-Lue et al. (Article in press). They use the R123 CLOHP with 1.06 and 2.03 diameters respectively. The evaporator lengths are 50, 100 and 150 mm. The numbers of turns are 5, 10 and 15.

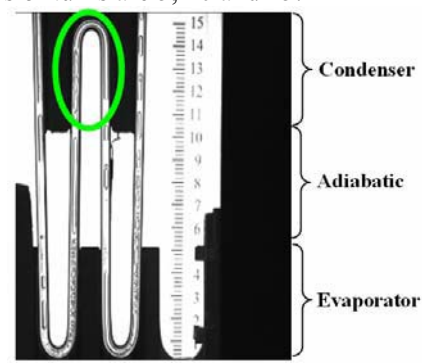


Fig.3 shown incomplete condensation in CLOHP

Heating of CLOHP was done by passing current to wall of evaporator section directly. Cooling of CLOHP was done by cooling water. The average surface temperature using in calculation of PCDC is determined from the average value of experimental temperature at evaporator and condenser section.

As method describe above, PCDC correlation is established by dimensional analysis of parameter involve the convection and phase change inside CLOHP. Hence the correlation is as follow,

$$S = 0.0133 \begin{bmatrix} Bo_{mix}^{0.65} \Pr_{mix}^{0.05} \operatorname{Re}_{mix}^{0.31} (\frac{NLe}{Di})^{2.15} \end{bmatrix}^{0.2893}$$
(25)

Start

Input outside surface temperature T_{cs} and T_{ds} .

Input geometry of CLOHP

Trial heat transfer rates (Q_0)

Calculate Z_0 from $\operatorname{eq.}(5)$

Calculate Z_0 from $\operatorname{eq.}(6)$

Calculate Z_0 from $\operatorname{eq.}(2)$

Calculate Z_0 from $\operatorname{eq.}(22)$

Calculate Z_0 from $\operatorname{eq.}(23)$

Calculate Z_0 from $\operatorname{eq.}(23)$

Calculate Z_0 from $\operatorname{eq.}(24)$

Calculate Z_0 from $\operatorname{eq.}(24)$

Calculate Form $\operatorname{eq.}(24)$

Calculate PotDC from $\operatorname{eq.}(24)$

Calculate Form $\operatorname{eq.}(24)$

Calculate PotDC from $\operatorname{eq.}(24)$

Calculate PotDC from $\operatorname{eq.}(24)$

False

Finish

Fig.4 Calculation flow chart

3. CALCULATION FLOW CHART

The determination of CLOHP heat transfer rate can be done as shown in figure 4. The calculation uses the iteration technique. The trial average heat transfer rates will be firstly assumed. This value was used to determine all of thermal resistance and thermodynamics property of working fluid. The calculated average heat transfer rates will

be determined by using above information. The calculation will finish when the assumed value is equal to the last calculated value. If these values are not equal, the trial value is set equal to the last calculated values.

4. RESULT AND DISCUSSION

4.1 Accuracy of CLOHP heat transfer rates prediction

Figure 5 show the comparison between the heat transfer rates from model and experimental data. We can see that the predict values by using this model give a good agreement with experimental data with ± 19.60 % error range.

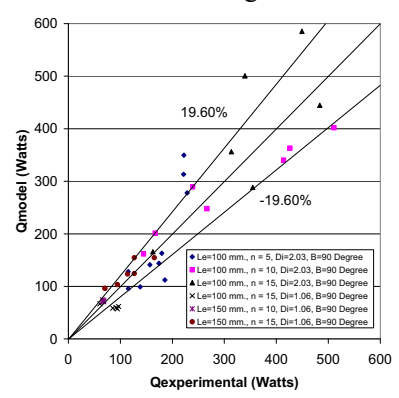


Fig.5 the accuracy of model in this paper

4.2 Effect of inside diameter on CLOHP heat transfer rates

Figure 6 shows the effect of inside diameter on CLOHP heat transfer rates. Experimental data of Charoensawan et.al. [1] and Kummuang-Lue et al. The prediction of model as shown in solid line shows that the average heat transfer rates increase linearly with inside diameter. The result from model agrees with both experimental data. However, there are different between both data. This is because, at normal operation, there are many heat transfer rates at the same working temperature. It depends on the temperature difference between evaporator and condenser surface. Thus, it is possible that Chroensawan's data is different from Kummuang-Lue et al. at the same diameter. All experimental procedures were done by controlled the operation at same adiabatic temperature. Their idea is represent the adiabatic section's temperature as working temperature. But we know that there are many values of heat transfer rate at the same working temperature at normal operation. These data, thus, may be obtained from same operating temperature unlike temperature difference between evaporator and condenser surface. Now it is too quick to conclude that increasing of inside diameter is result in increasing of heat transfer rate. Figure 7 show the inner thermal resistance, values of Z₃, Z₄, Z_5 and Z_6 calculated from model, at several of inside diameter and fix others parameter. We can see that

there are slightly change in inner thermal resistance when inside diameter changed. Moreover, the inner thermal resistance increases with diameter in diameter range of 0.006 - 0.001 m while it is decrease in range of 0.001 - 0.002 m. This is because the competition between the Z_3 and Z_4 in evaporator, also Z₅ and Z₆ in condenser section. In case of increasing inside diameter, the circulation velocity decreased result in increasing of Z3 and Z6, while it approach pool boiling result in decreasing of Z_4 and Z_5 . However, if we consider the order of magnitude of change in inner thermal resistance, we can say that it is slightly change in values. Both tendencies in figure 6 and figure 7 are correct but in different situation. The result shown in figure 6 is usually met in actual experiment because it is too difficult to control the both working temperature and temperature different at the same condition and vary inside diameter. Thus, we can conclude that the model can efficiently predict both above situation. The model shows that the change in inner diameter results in slightly change of inner thermal resistance. The increasing of heat transfer rates with inner diameter can be found in case of maintains working temperature at constant and temperature different between evaporator and condenser surface is difficult to control as constant value.

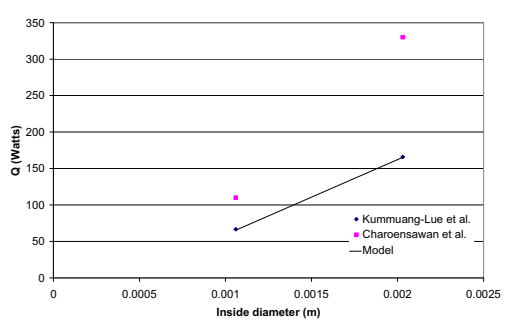


Fig.6 effect of diameter on heat transfer rates

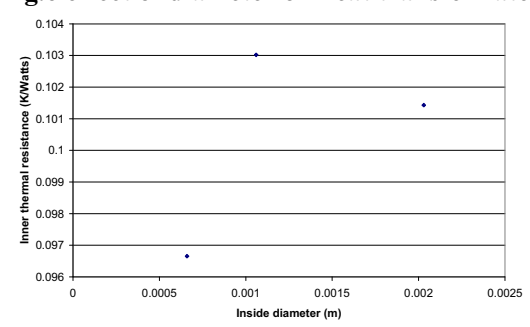


Fig.7 Inner thermal resistance at several of ID 4.3 Effect of evaporator length on CLOHP heat transfer rates

Figure 8 shows the effect of evaporator length on heat flux transfer rates. We can see that the average heat flux from the model decreases with increasing of evaporator length. This is because increasing of evaporator length results in increasing of inner thermal resistance. Charoensawan et al. [2]

discuss the effect of evaporator length on heat flux transfers that when the evaporator length increased, the amplitude of oscillation is high but low in frequency. Charoensawan's statement in aspect of this model means that when the evaporator length increases, the velocity of circulation decrease. This results in increasing of Z_3 and inner thermal resistance. Thus heat flux transfer will decreased with increasing of evaporator length. It can be conclude that this model agree with Charoensawan's result and heat flux transfer decreased with increasing of evaporator length.

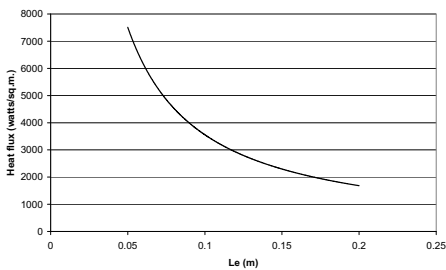


Fig.8 the effect of evaporator length on heat flux transfer rates

4.4 Effect of number of turns

Figure 9 shows the effect of number of turns on heat flux transfer rates. We can see that the average heat transfer rates from the model decrease with number of turns. This result agrees with Charoensawan et al.[2] and Khummuang-Lue et al. However, these experimental data are obtained by maintaining constant working temperature. As previous discussion, the heat transfer rate may be more than one value for given operating temperature. Thus figure 9 is a one possible way to predict the effect of evaporator length on the heat transfer rate. Figure 10 shows the effect of number of turns on heat flux transfer rate by using result from this model. The calculation is done by fixing all parameters except number of turns. We can see that the heat flux transfer slightly increases with number of turns. This is because the increasing of turns result in increasing of convective surface area and number of pool boiling. The superposition of both factor results in increasing of heat transfer rates with turns. This result disagrees with above experimental data because the temperature difference between evaporator and condenser surface is maintain constant in model while there are a change in above experimental data. However, it is not possible to fix both temperature difference and operating temperature in actual experiment. Thus the result in figure 9 and 10 are both correct but are in different situation. Thus it can be concluded that the heat flux transfer is slightly increase with number of turns in case of fix all parameter except number of turns, while in actual experiment we usually see that the heat flux transfer is decrease with number of turns.

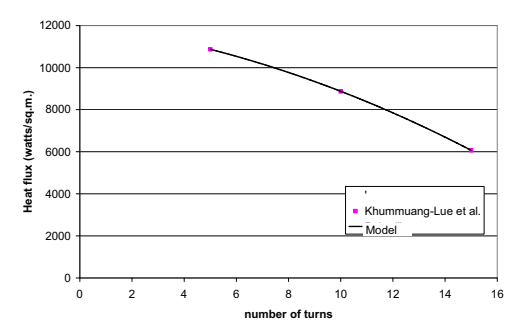


Fig.9 the effect of turns on heat transfer rates

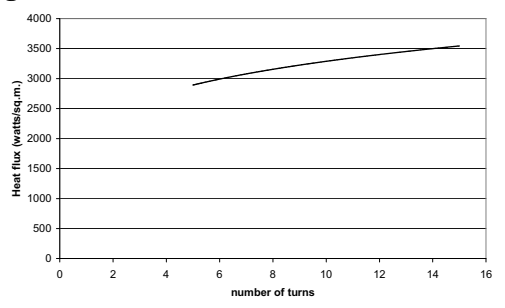


Fig.10 effect of turns on heat transfer rates 5. CONCLUSION

The model for prediction of the CLOHP average heat transfer rates by using the concept of average thermal resistance were successfully created in this paper with ± 19.60 % error range comparing with the experimental data. The model indicated that heat transfer rates are increased with inner diameter. Heat flux transfer decreased with increasing of evaporator length and slightly increase with number of turns in case of fix all parameter except number of turns, while in actual experiment we usually see that the heat flux transfer is decrease with number of turns. The PCDC was introduced to represents the specific characteristic of CLOHP.

Acknowledgement

All of this work cannot be conducted without the support from the Thailand Research Fund (Contract no. BRG4780024). The authors would also like to express their sincere appreciation.

References

- Charoensawan, P., Khandekar, S., Groll, M., and Terdtoon, P., Closed Loop Pulsating Heat Pipe Part A: Parametric Experimental Investigations. Applied Thermal Engineering. Vol. 23., 2003.
- Charoensawan, P., Terdtoon, P., Tantakom, P., and Ingsuwan, P., Effect of Evaporator Section Lengths, Number of Turns and Working Fluid on Internal Flow Patterns of a Vertical Closed-Loop Oscillating Heat Pipe. Procs. of the 7th International Heat Pipe Symposium. Jeju Korea., 2003.
- Dobson, R.T., and Harms, T.M., Lumped Parameter Analysis of Closed and Open Oscillatory Heat Pipe. Procs. of the 11th International Heat Pipe Conference. Tokyo Japan., 1999.
- Dobson, R.T., and Graf, G., Thermal Characterisation of an Ammoniacharged Pulsating Heat Pipe. 7th International Heat Pipe Symposium. Jeju Korea., 2003.
- Maesawa, S., Heat Pipe: Its Origin, Development and Present Situation. Procs. of the 6th International Heat Pipe Symposium. Chiang Mai Thailand., 2000
- Shafii, M., Faghri, A., and Zhang, Y., Thermal Modeling of Unlooped and Looped Pulsating Heat Pipes. Journal of Heat Transfer. Vol.123., 2001.
- Wong, T.N., Tong, B.Y., Lim, S.M., and Oci, K.T., *Theoretical Modeling of Pulsating Heat Pipe*. Procs. of the 11th International Heat Pipe Conference. Musashinoshi Tokyo Japan., 1999.

ภาคผนวก ง

บทความ

EFFECT OF EVAPORATOR LENGTHS AND WORKING FLUID ON HEAT TRANSFER CHARACTERISTIC OF AN INCLINED CLOSED-END OSCILLATING HEAT PIPE AT CRITICAL STATE

EFFECT OF EVAPORATOR LENGTHS AND WORKING FLUID ON HEAT TRANSFER CHARACTERISTIC OF AN INCLINED CLOSED-END OSCILLATING HEAT PIPE AT CRITICAL STATE

T. Hudakorn, P. Sakulchangsatjatai, K. Buddajun* and P. Terdtoon

Department of Mechanical Engineering, Faculty of Engineering, Chiang Mai University Thailand.

Tel. +66 53 944146, Fax +66 53 226014, E-mail: hudakorn_t@hotmail.com
* Department of Mechanical Engineering, Faculty of Industrial technology and management,

King Mongkut's Inst. of Technology North Bangkok Thailand.

Abstract

This study presents the effect of the evaporator section lengths and working fluid properties on heat transfer characteristic of an inclined close – end oscillating heat pipe (CEOHP) at critical state. The CEOHP was made of copper tube with the evaporator length of 50, 100 and 150 mm, inner diameter of 2.03 mm. and number of meandering turn of 10. For each CEOHP, the length of the condenser, adiabatic and evaporator sections were set at equal length. The working fluids used were R123, ethanol and water with a filling ratio of 50% of total volume of the tube. The experiments were conducted by setting the inclination angles at 0 – 90 adjusted by 10 degree, with controlled vapor temperature of $60\pm5^{\circ}$ C. It was found from the experimental that the evaporator section lengths and latent heat of evaporation affected on $Q_c/Q_{c,90}$.

KEY WORDS: Closed- end oscillating heat pipe, heat transfer characteristic at critical state

1. Introduction

Recently, electronic devices dominating in everyday life such as computer and electric devices which have well heat removal requirement. For example, using the cooling fan system results in heat accumulation and consequently shorter life period. Conventional heat pipe is used to solve this problem. So that, its required size is smaller as would be needed to install in heat removal area constraint. It has also several limitations i.e. the capillary limit which is dominate when the wick structure cannot return with enough amount of liquid back to the evaporator section. The entrainment limit is due to the counter flow effects of the vapor and liquid condensation. To solve this problem, Akachi et. al (1994) invented a new type of heat pipe called oscillating heat pipe.It has a simple structure in contrast with conventional heat pipe because there is no wick structure to return condense liquid from the condenser section to the evaporator section. The OHP is made from a continuous long capillary tube bent into many turns and filled with some working fluids. The inner diameter of the OHP must be sufficiently small so that vapor plugs and liquid slugs can be formed [7]. The OHP can operate successfully for any operation modes. The vapor plugs, and the phase changes of working fluid inside tube. There are three basic types of OHP varying on its configuration: first, close-end OHP (CEOHP) which is closed both ends in each. Second, close-loop OHP (CLOHP) which is connected at both ends of tube to form loop. Finally, Close-loop OHP with check valve (CLOHPWCV) in which a check valve is installed at the loop.

At present, there are a lot of studies on heat transfer characteristics of OHP at normal operating condition [1, 6, 8, 9]. But in operational condition, it has a limitation of heat transfer capability. Very few studies have investigated on it, which will be mentioned as follow. Maezawa et. al. (1996) observed that, at a specific condition of their experimental works, the dryout occurred only at evaporator section and the CEOHP did not operate. Lin et. al. (2000) found that inadequate fill ratio easily led to the dry out condition because it was caused by the insufficient quantity of liquid inside the evaporator section. It can be observed from past researches that dry out will occur at evaporator section. Therefore, Katpradit et. al. (2003) established his hypothesis to explain these phenomena which can be illustrated in Fig. 1. When the CEOHP is heated to some degrees, internal thermal resistance will rapidly increase. The heat flux from the evaporator to condenser section cannot accordingly be transferred, and the outside surface temperature subsequently increases to unlimited level. The inside vapor pressure is subsequently high. This high vapor pressure will retard the liquid slug from returning back to the evaporator section. The liquid quantity in the evaporator section is accordingly small and this caused the dry out at some part of the evaporator. The state at which the dry out occurs is called "Critical State" of OHP.

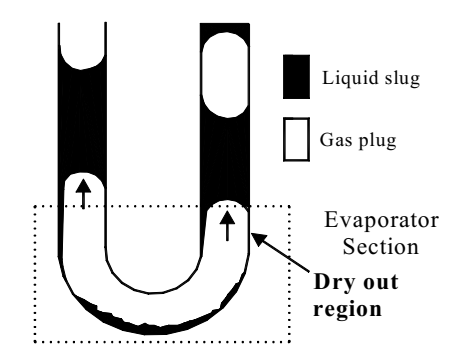


Figure 1 Dry out occurred at evaporator section.

Anuchitchanchai et al. (2003) studied the effect of aspect ratio and internal diameter on critical heat flux using MP39 and HP62 as working fluids. It was found from the experiment that the critical heat flux decreased as the aspect ratio increased and increased as the internal diameter of the tube increased. Panyoyai et al. (2004) studied the effects of meandering turns and aspect ratios on internal flow patterns of CEOHP at critical state. It was found that dryout was caused by flooding at the top of evaporator show in Fig. 2, which supported hypothesis of Katpradit et. al. (2003)

Moreover, Katpradit et. al. (2005) found the correlation to predict critical heat flux at vertical and horizontal orientation as follow

$$Ku_{_0} = 53680 \times \left[\frac{Di}{Le}\right]^{1.127} \times \left[\frac{Cp\Delta T}{h_{\mathrm{fg}}}\right]^{1.417} \times \left[Di\left[\frac{g\left(\rho_{_{\mathrm{v}}} - \rho_{_{1}}\right)}{\sigma}\right]^{0.5}\right]^{-1.32}$$

$$Ku_{90} = 0.0002 \times \left[\frac{Di}{Le}\right]^{0.92} \times \left[\frac{C\rho\Delta T}{h_{fg}}\right]^{-0.212} \times \left[Di\left[\frac{g(\rho_{v} - \rho_{t})}{\sigma}\right]^{0.5}\right]^{-0.59} \times \left[1 + \left(\frac{\rho_{v}}{\rho_{t}}\right)^{0.25}\right]^{13.062}$$

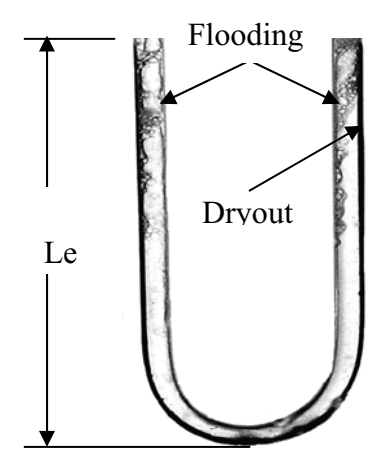


Figure 2. Visualization of dry out occurred at evaporator section

It was found from dimensionless analysis that the vertical heat mode have dimensionless parameter of Wallis or Wallis number $(1+(\rho_v/\rho_1)^{0.25})$, Wa), which used to explain the flooding phenomena that influent the dryout occur at evaporator section. Hudakorn et al. (2004) studied the inclination angle on heat transfer characteristic of a CEOHP at critical state. It was found from the experiment that the Q_c/Q_{c,90} increases from 1 to 1.52 as the inclination angle decreases from 90 to 60 and $Q_c/Q_{c,90}$ decreases from 1.48 to 0.25 when the inclination angle decreases from 40 to 0. The maximum Q_c/Q_{c,90} occurs in the range of inclination angle of 40 - 60 degree.

It can be obviously observed from the past researches that the effect of evaporator length and working fluid property on performance limit of the inclined CEOHP is not fully understood. Therefore, the objectives of this research are as follows

- 1. To clarify effect of evaporator length and working fluid on critical heat flux of inclined CEOHP
- 2. To experimentally investigate the effect of evaporator length and working fluid on heat transfer characteristics of a inclined CEOHP at critical state.
- 3. To compare our results with critical heat flux of the CEOHP which was studied in the past.

2. Experimental set up and procedure

The schematic diagram of the experimental setup is shown in Figure 3. It consists of the CEOHP, an AC high-current low-voltage power supply (6,000A, 0.6V), a cooling bath, a data logger (Brainchild, VR18, and \pm 0.5°C), and a flow meter (Platon, PGB411, and \pm 0.1 lit/min.). The CEOHP is made from a copper capillary tube bent to a series of undulating turns. The separated of two bus bars are attached by welding at its lower part that defines the evaporator length, Le. The current from a high-current low-voltage power supply is passed from one bus bar, through the copper tube, to the other bus-

bar, the medium by which heat was generated from the electrical resistance of the tube itself. The mixture of water and ethylene - glycol 50% by volume is circulated from the cooling bath through the cooling jacket to remove the heat out of the condenser section. The adiabatic section of the CEOHP is insulated.

Eighteen Chromel-Alumel thermocouples (Omaga, K type, \pm 0.5°C) were placed on the CEOHP wall: ten in middle of the evaporator section, four in middle of the adiabatic section and four in middle of the condenser section. In addition, four points of thermocouples were used to measure the temperature of the cooling solution: two at the inlet and two at the outlet section of condenser to monitor the temperature difference to calculate the heat transfer at critical state by using the calorific method, as the following equation;

$$Q = \dot{m}C_{p} \left(T_{out} - T_{in} \right) \tag{1}$$

Where

 \dot{m} = Mass flow rate of the cooling solution

 c_n = Specific heat of the cooling solution

 $(T_{out} - T_{in})_c$ = Temperature different of inlet and out let of the cooling solution

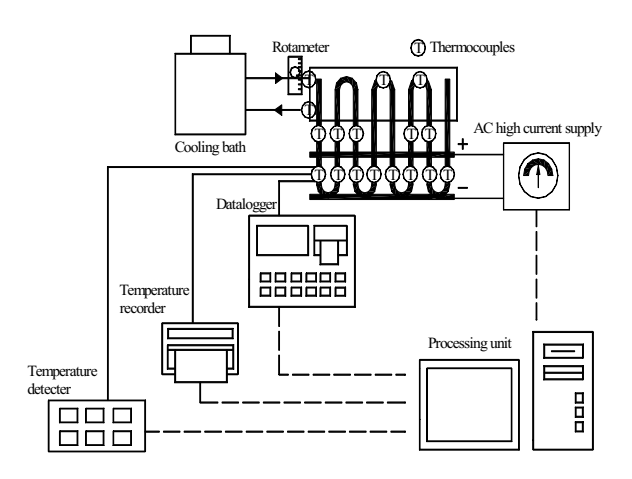


Figure 3 Experimental setup

The steps to find the heat transfer at critical state were follows, the heat was gradually added to the CEOHP at the evaporator section in small step by adjust a variac and the heat was removed at the condenser section by a calorific jacket with cooling substance. Then, the temperature at adiabatic section was maintained at 60±5°C by adjusting the flow rate and/or the cooling temperature for different the input power. At

steady state, the temperature at each point on the evaporator section, flow rate and input power data were recorded. The rate of heat transfer was calculated from the difference of inlet and outlet temperatures at the condenser section by the calorific method. The wall temperatures in each tube of the evaporator section were compared. The procedure was repeated by increasing voltage until one or more wall temperature at the evaporator section started to increase rapidly due to the vapor pressure at evaporator section. This high vapor pressure will retard the returning condensate liquid film from condenser section to the evaporator section. The liquid quantity in the evaporator section is accordingly small and this causes dryout at the evaporator section. The state at which the dry out occurs is identified as "Critical State", show in figure 4.

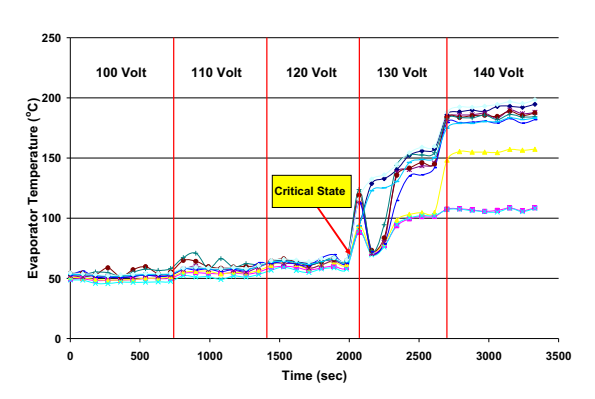


Figure 4 wall temperature profiles at evaporator section of CEOHP (D = 2.03 mm, Le = 100 mm, Turn = 10, R123, $\beta = 90^{\circ}$)

In order to study the effect of evaporator length and working fluid on heat transfer characteristics of a inclined CEOHP at critical state. The controlled parameters were as follows:

- Inner diameter of 2.03 mm. (This inner diameter of the CEOHP was sufficiently small so that vapor plugs and liquid slugs can be internally formed)
- Number of turn of 10. (To compare our results with researches studied in the past)
 The variable parameter was:
- Evaporator lengths were 50, 100 and 150 mm.
- Working fluid were R123, ethanol and water
- Inclination angle were 0 90 degree (adjust by 10 degree).

In calculation of the heat transfer at critical state by equation (1), the accumulated error of obtained heat transfer could be determined by

$$dQ = \left(\frac{\partial Q}{\partial \dot{m}} d\dot{m} \right)^{2} + \left(\frac{\partial Q}{\partial T_{out}} dT_{out} \right)^{2} + \left(\frac{\partial Q}{\partial T_{out}} dT_{out} \right)^{2}$$

$$\left(\frac{\partial Q}{\partial T_{in}} dT_{in} \right)^{2}$$

$$(2)$$

Where

dq = error of the heat transfer at critical state

 $d\dot{m}_c$ = accuracy from measuring the mass flow rate of cooling solution

 $dT_{c,in}$ = accuracy from measuring the inlet temperature

 $dT_{c,out}$ = accuracy from measuring the outlet temperature

3. Result and discussion

From the experimental, it can be observed that the dryout phenomenon first occurred at the evaporator section in turn of the sealed ends of tube. After more heat was supplied, dryout occurred anywhere within evaporator section. In this study, the critical heat flux was calculated at the point where the first dryout occurred. The dryout was detected by monitoring the temperature of evaporator section. The experimental results can be present as follows:

3.1 Effect of evaporator length

In all experiment, the evaporator and condenser section were setting equal length because the heat flux at evaporator and condenser of CEOHP was also equal. The effect of evaporator section length on the critical heat flux is shown in Fig.5.

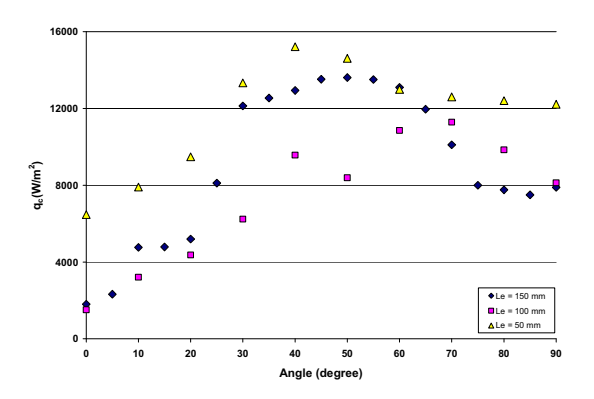


Figure. 5 Effect of Evaporator length on critical heat flux at any angle of CEOHP (Di = 2.03 mm. Turn = 10, R123)

From the Fig 5, it can be divided into 2 range of operating orientation;

- 1. The range of 70 to 90 and 0 degree, this operating orientation found that the evaporator length increased as the critical heat flux decreased. From this range, the result of experiments was compare with data from Katpradit et. al. (2005). It was found that the critical heat flux decreased as the evaporator length increased. This is in good agreement with the result from this study. A possible explanation is that when the evaporator length increases, the vapor plug that form inside the tube is longer and the vapor bubbles do not easily move to the condenser section. In addition, the liquid inside the vapor bubbles will quickly evaporate to the condenser section and hold the liquid that returns from condenser back to evaporator section. For this reason, the long evaporator section easily to occur dryout cause by the critical heat flux decreased.
- 2. The range of 10 to 70 degree, it can be seen that the 100 mm. of evaporator length have lower critical heat flux than 150 mm. of evaporator length. So that, this range the evaporator length doesn't affect on critical heat flux.

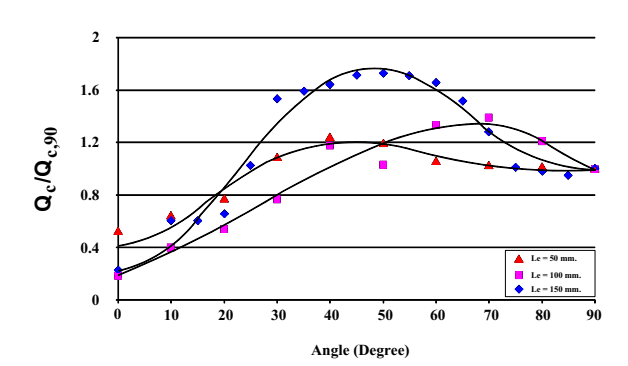


Figure. 6 Effect of Evaporator lengths and the inclination angle on $Q_c/Q_{c.90}$ (Di = 2.03 mm. Turn = 10, R123)

In the case of an inclined of CEOHP, to eliminate the effect of many parameters involved in the heat transfer mechanism, it is necessary to normalize the critical heat transfer rate of inclination angle with the critical heat transfer rate at vertical position $(Q_c/Q_{c.90})$, show in Fig. 6.

Form Fig.6, the tendency of $Q_c/Q_{c,\ 90}$ all evaporator lengths is bell shape but the maximum $Q_c/Q_{c,\ 90}$ are different in each angle. Form the result; it was found that the evaporator length increase from 50 to 150 mm. as the maximum $Q_c/Q_{c,\ 90}$ increase. This might be because the higher evaporator length has more surface area which is used to transfer the heat. The maximum $Q_c/Q_{c,\ 90}$ were 1.25, 1.39 and 1.73 respectively.

3.2 Effect of working fluid

Figure 7 shows Effect of working fluid on critical heat flux at any angle of CEOHP.

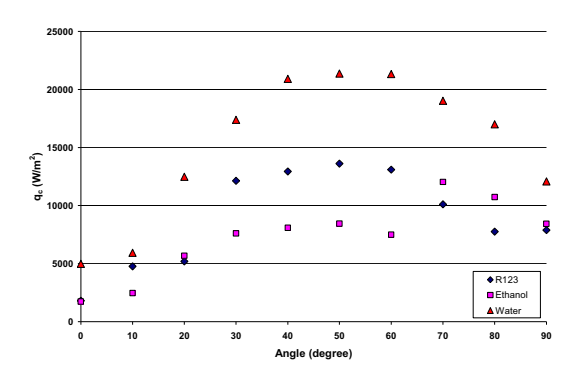


Figure 7 Effect of working fluid on critical heat flux at any angle of CEOHP.

(Di = 2.03 mm. Le = 150 mm. Turn = 10)

From the Fig 7, it can be divided into 2 range of operating orientation;

1. The range of 70 to 90 and 0 degree, this range found that the latent heat of vaporization increased as the critical heat flux increased. It was found from the experiment that R123 has lower critical heat flux compared ethanol and water. This might be because, when heated, R123 vaporizes with a higher vapor pressure at evaporator section, and the working fluid in condenser section quickly retarded by the high vapor pressure at evaporator, causing insufficient liquid supply to evaporator section, as a result dryout occurs. From this range, the result of experiments was compare with data from Katpradit et. al. (2005). It was found that the critical heat flux increased as the latent heat of vaporization increased. This is in good agreement with the result from this research. Moreover, the obtain data was also in agreement with Lin et al. (2000), which found that FC - 72 (lower latent heat of vaporization) had a lower critical heat flux than FC - 75 (higher latent heat of vaporization).

2. The range of 10 to 70 degree, it can be seen that the latent heat of vaporization does not affect on critical heat flux.

Figure 8 shows Effect of working fluid on $Q_c/Q_{c,90}$ at any angle of CEOHP.

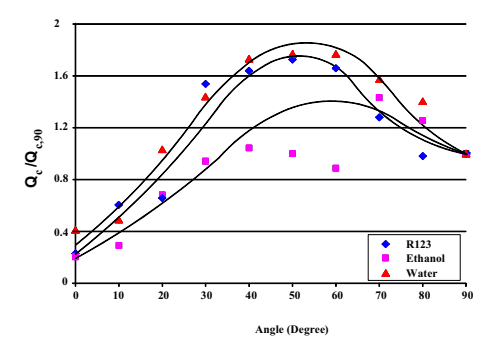


Figure 8 Effect of working fluid on $Q_c/Q_{c, 90}$ at any angle of CEOHP. (Di = 2.03 mm. Le = 150 mm. Turn = 10)

Form Fig.8, the tendency of Q_c/Q_c , 90 of R123, ethanol and water is bell shape and the maximum Q_c/Q_c , 90 are nearly the same in range of 50-70 degree. This is because in this range, the shear stress between vapor plugs and liquid film and the body force of the liquid film are major factor. The maximum Q_c/Q_c , 90 were 1.43, 1.73 and 1.77 for ethanol, R123, and water respectively. It can be seen that the latent heat of vaporization is not only major factor in the heat transfer mechanism. This might be depending on other factor of working fluid property such as surface tension, liquid density, vapor density specific heat and dynamic viscosity of working fluid.

4. Conclusion

Effect of evaporator length and working fluid on heat transfer characteristic of an inclined CEOHP at critical state has been experimentally investigated and it was found that the evaporator section lengths and latent heat of evaporation affected on $Q_c/Q_{c,90}$.

5. Acknowledgement

All of this work cannot be conducted without the support from the Thailand Research Fund (Contract no. BRG4780024). The authors would also like to express their sincere appreciation.

References

- 1. Akachi, H., Polasek, F., and Stulc, P., *Pulsating Heat Pipe*. Procs. of the 5th International Heat Pipe Symposium. Melbourne Australia., 1996.
- Anuchitchanchai, P., Kamonpet,
 P., Wongratanaphisan, T., and Terdtoon, P.,
 Effect of Aspect Ratios and Internal Diameter
 on Performance Limit of A Closed-End
 Oscillating Heat Pipe Using Refrigerant Blend
 as Working Fluid. Procs. of the 7th International
 Heat Pipe Symposium. Jeju Korea, 2003.
- 3. Hudakorn, T., Budhajan, K., Chareonsawan, P., Waowaew, S. and Ritthidech, S., *Effect of Inclination Angle on Heat Transfer Characteristic of A Closed End Oscillating Heat Pipe at Critical State.* 1 st International Seminar on Heat Pipes and Heat Recovery System. Kuala Lumpur Malaysia, 2004.
- Katpradit, T., Wongratanaphisan, T., Terdtoon, P., Akbarzadeh, A., and Kamonpet, P., Correlation to predict Heat Transfer Characteristics of A Closed End Oscillating Heat Pipe at Critical State. Applied Thermal Engineering, 2005.
- Kapradit, T., Kamonpet, P., Wongratanaphisan, T., and Terdtoon, P., Effect of Number of Turns and Working Fluids on Heat Transfer Characteristics of A Closed-End Oscillating Heat Pipe at Critical State. Procs. of the 7th International Heat Pipe Symposium. Jeju Korea, 2003.
- Lin, L., Ponnappan, R. and Leland, J.,
 Experimental Investigation of Oscillating
 Heat Pipe. 35th Energy Conversion
 Engineering Conference and Exhibit. Vol. 2,
 2000.
- Maesawa, S., Gi, K.Y., Minamisawa, A., and Akachi, H., *Thermal Performance of Capillary Tube Thermosyphon.* Procs. of the IX International Heat Pipe Conference. Albuquerque USA. Vol. II, 1996.
- 8. Panyoyai., N., Effect of Meandering Turns and Aspect Ratio on Internal Flow Patterns of Closed End Oscillating Heat Pipe at Critical State. Thesis for Master of Engineering in Mechanical Engineering, Chiang Mai University, 2004.
- Ritidech, S., Terdtoon, P., Tantakom, P., Murakami, M., and Jompakdee, W., Effect of Inclination Angles, Evaporator Section lengthes and Working Fluid Properties on heat Transfer Characteristics of A Closed – End Oscillating Heat Pipe. Procs. of the 6th International Heat Pipe Symposium. Chiang Mai Thailand., 2000.

 Ritidech, S., Terdtoon, P., Murakami, M., Tantakom, P., and Jompakdee, W., Correlation to predict heat transfer characteristics of a closedend oscillating heat pipe at normal operating condition. Applied Thermal Engineering. Vol. 23., 2003

ภาคผนวก จ

บทความ

Time Response Model of Operational Mode of Closed-Loop Oscillating Heat Pipe at Normal Operating Condition

Time Response Model of Operational Mode of Closed-Loop Oscillating Heat Pipe at Normal Operating Condition

N. Soponpongpipat, P.Sakulchangsatjatai, M.Saiseub and P. Terdtoon*

Department of Mechanical Engineering, Faculty of Engineering, Chiang Mai University, Thailand 50200.

Tel. +66-53-944151 Fax. +66-53-226014 Email: Nitipongsopon@hotmail.com

* Presenter

Abstract

This paper shows the new assumption of CLOHP at normal operating condition. The evidence from visual study showed the possibility that CLOHP entirely operated at constant values of pressure. The main mechanism which driving the working fluid flow inside CLOHP is "replacement process". The study indicated that the time series heat transfer characteristic of CLOHP depends on condensation and evaporation rates of working fluids. The rate of phase change in a certain time will effect on the rate in the next time. Finally, this paper shows the alternate direction of circulation mechanism inside CLOHP. This mechanism is not the result from the change in pressure wave but it is the result from the effect of incomplete condensation. The incomplete condensation changes the direction of vapor replacement and consequently changes in direction of circulation.

Key Words: CLOHP, Time Response Model

1. INTRODUCTION

Closed Loop Oscillating Heat Pipe (CLOHP) is one type of heat pipe. Because of its small size and wickless structure, CLOHPs are interested in electronics cooling application. **CLOHP** constructed by meander the capillary tube and connect its both ends together. Due to complexity of its operation, there are many research study the operation principle and heat transfer behavior of CLOHP. In aspect of quantitative study, Charoensawan et al. [1] studied the effect of tube geometry and types of working fluid on CLOHP heat transfer rates. In aspect of qualitative study, there were research about the effect of tube geometry, types of working fluid and filling ratio on internal flow pattern inside CLOHP [3,4,5]. Many research indicate that the circulation of working fluid inside CLOHP due to either pressure different between each turn or change in pressure wave. In aspect of mathematical model, Dobson et al. [2] presented the behavior of vapor slug inside CLOHP by using the ideal gas law.

Many researches explain the cause of circulation that due to the expansion and collapse of vapor slug under pressure difference between condenser and evaporator section in each turn. Are there any possibilities that the vapor slug expands and collapses under the constant pressure? Can we say that the expansion and collapse process under quasi static condition? The answers of these questions lead to the new assumption of CLOHP modeling and good understanding of CLOHP behavior. Thus in this paper, the data from visual study will be considered and be made logical analysis in order to show the possibility that the cause of circulation inside CLOHP is the expansion and collapse under constant pressure. Moreover, the

expansion of vapor slug is result from evaporation of around liquid into vapor slug rather than the ideal gad law expansion. This new assumption is advantage in explanation of CLOHP operation.

2. DATA FROM VISUAL STUDY

Visual study data in this paper gather from Sakulchangsatjatai et al. (Article in press). The experiment was conducted by using the 2 turnsplexiglass CLOHP. The working fluid was R123. Electric heater was used as heat source. The heating mode was bottom heat. Heat passed to CLOHP by conduction through the high conductivity silicone paste. The silicone was pasted between heater and CLOHP. Water was use as cooling medium. The evaporator, adiabatic and condenser length is 50 mm. The working temperature is maintained at 220°C. The visual study data were taken by highresolution charge-coupled device (CCD) still camera of speed 30 images per second with one million pixels resolutions. The flow pattern inside CLOHP will be observed continuously until experiment is over. The evaporator section is located at the bottom of still picture while the condenser section is at the top of still picture. In picture, the vapor phase is clearer than the liquid phase. By using the boundary line and the clarity, we can separate the vapor phase from liquid phase.

3. RESULT AND DISCUSSION

3.1 The expansion of vapor slug at evaporator section

The necessary condition for normal operation mode of CLOHP is the inner surface of CLOHP at evaporator section will be coated with liquid all the time. Otherwise, the surface will have a high temperature rapidly. This is because the

thermal conductivity of vapor is much lower than liquid. Thus, it is difficult for vapor to remove heat from inner heating surface. As above mention, it is clear that there are not any vapor slug contacts with heating surface directly. In contrast, there are liquid between vapor and heating surface as shown in figure 1

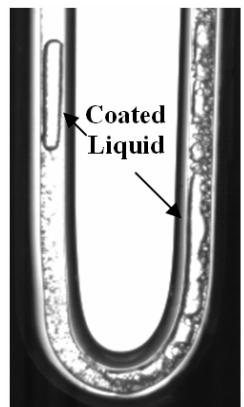


Fig. 1 shown the liquid film between vapor slug and evaporator surface

Heat transfer mechanism in normal operation mode can be explained as follow. The heating medium around CLOHP transfers heat to outside evaporator surface. Heat is transferred from outside surface to inner surface by conduction. Heat, later, is transferred to liquid which coated around inner surface by conduction and convection. Finally, coated liquid will transfer heat into vapor slug. Because of thermal conductivity of vapor is lower than liquid, it is clear that heat transfer from liquid to vapor by conduction is quite little. In this situation, in order to keep heat balance, coated liquid have to evaporate and move to increase volume of vapor slug. It is, therefore, distinct to say that heat can transfer from coated liquid to vapor slug by evaporation. The heat conduction from coated liquid to vapor slug is very low comparing with evaporation.

In addition, if we take more consideration about the necessary condition for normal operation mode and heat transfer mechanism discussed above, we can see that there are less possibilities for vapor to be superheat vapor. This is because the vapor slug does not directly receive heat from evaporator surface and the increasing of vapor volume is result from evaporation of liquid around it. Using of ideal gas law to explain behavior of vapor slug in CLOHP, therefore, is rather not suitable.

3.2 Operating Pressure inside CLOHP

One of the interested problems in this research is "Do CLOHPs transfer heat under a constant operating pressure entire the tube or under a two pressure difference, the difference between the pressure corresponding to evaporator temperature and the pressure corresponding to condenser temperature?" The answer of this question can be found from photographs of working fluid flow

pattern as shown in figure 2. The considered vapor slug in figure 2 is marked with ellipse. We can see from figure 2(a)-(d) that both ends of vapor slug shrink and move upward to the top side. This configuration indicates that the collapse of vapor slug is a result from condensation and the vapor has lower pressure than the evaporator pressure at the bottom side of figure. This is because the pressure occurred in each part will correspond to their temperature. The evaporator which has high temperature will also have high pressure. In the same way, the condenser will have both low temperature and pressure. The evaporator pressure will press the marked vapor slug. We, therefore, will see the marked vapor slug collapse in both sides. If we analyses as discuss above, it can be conclude that CLOHP operate with two different pressures.

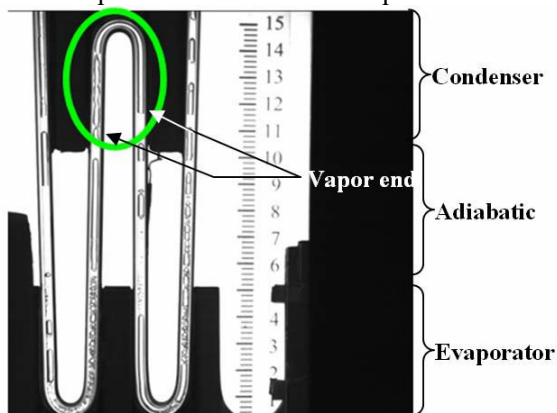


Fig. 2(a) flow pattern at t = 0 sec.

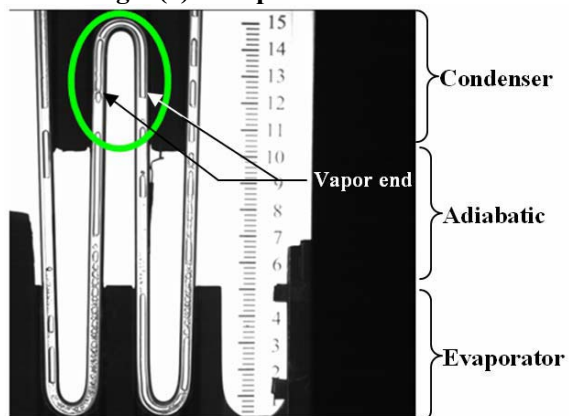


Fig. 2(b) flow pattern at t = 1/30 sec.

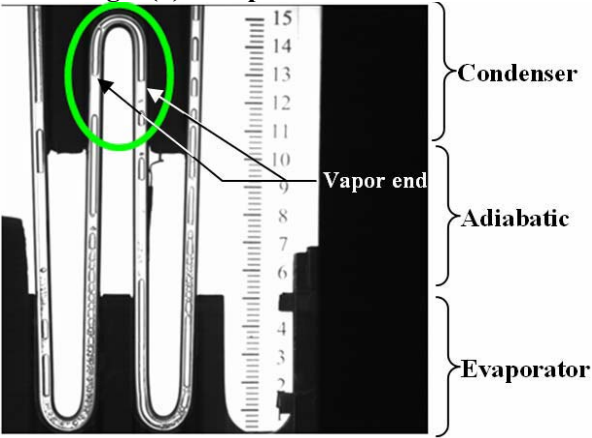


Fig. 2(c) flow pattern at t = 2/30 sec.

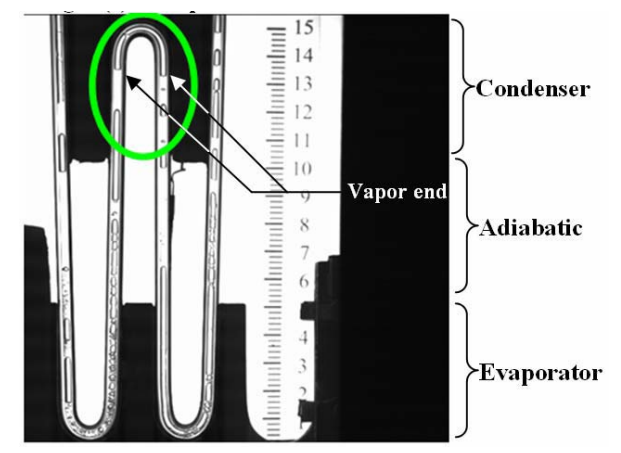


Fig. 2(d) flow pattern at t = 3/30 sec.

However, figure 2(e)-(j) show that both ends of the vapor do not shrink and move in same direction as discuss above. In contrast, its both ends shrink and move in opposite direction. This situation makes the assumption that CLOHP operate between two different pressure fail. One possible assumption about CLOHP operating pressure, thus, is CLOHP operate with constant pressure. The circulation of working fluid is result from vapor expansion in evaporator and collapse in condenser at constant pressure. The vapor volume in evaporator will expand to replace the condense volume in condenser under quasi-static process. The circulation, once again, does not result from pressure difference.

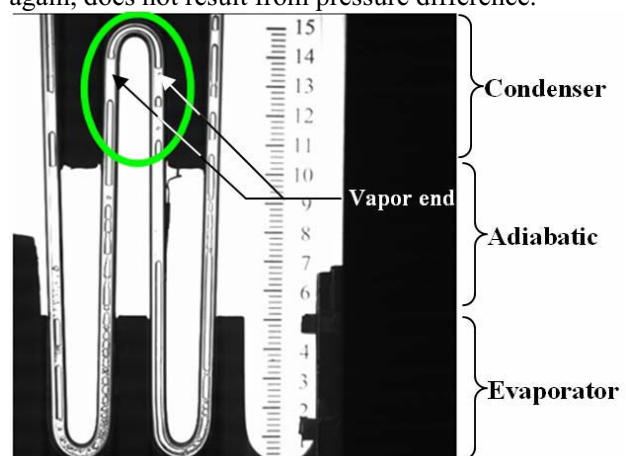


Fig. 2(e) flow pattern at t = 4/30 sec.

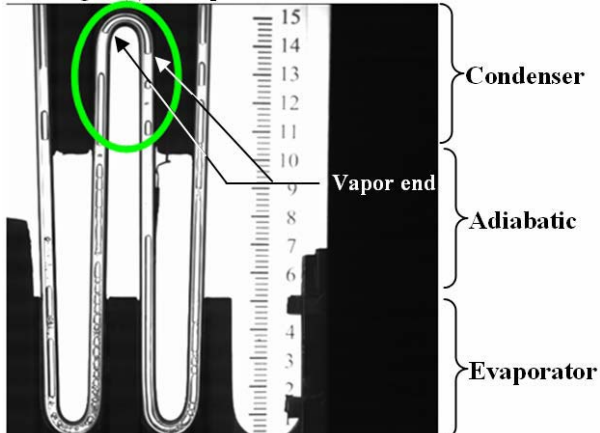


Fig. 2(f) flow pattern at t = 5/30 sec.

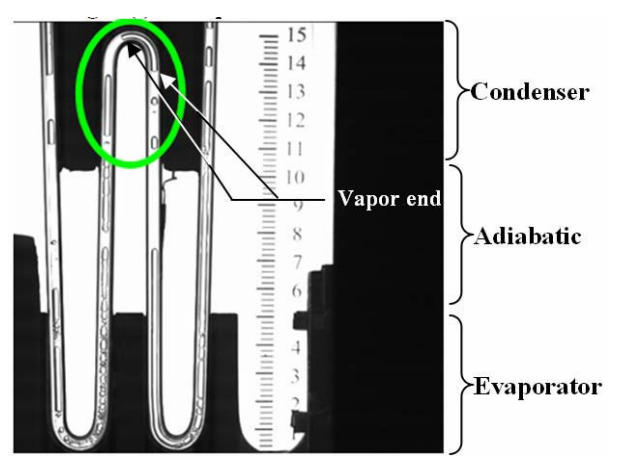


Fig. 2(g) flow pattern at t = 6/30 sec.

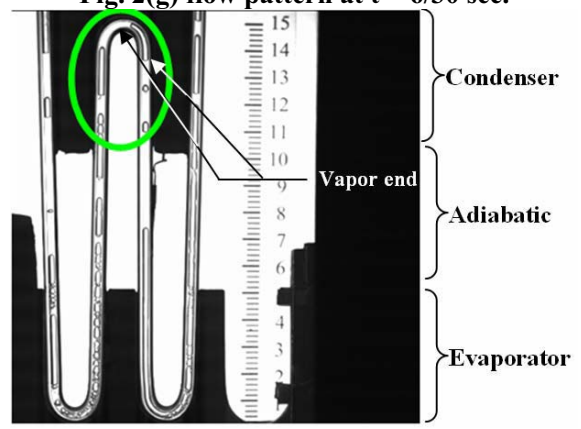


Fig. 2(h) flow pattern at t = 7/30 sec.

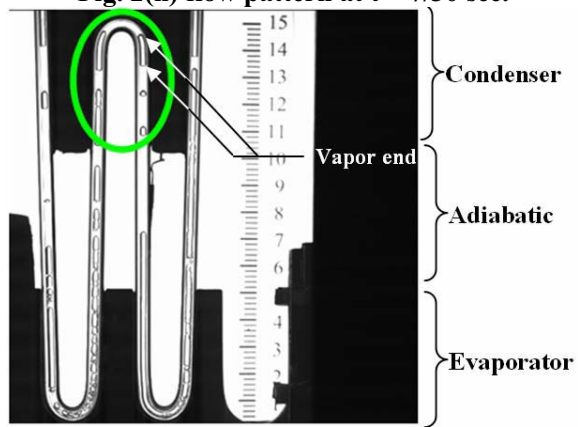


Fig. 2(i) flow pattern at t = 8/30 sec.

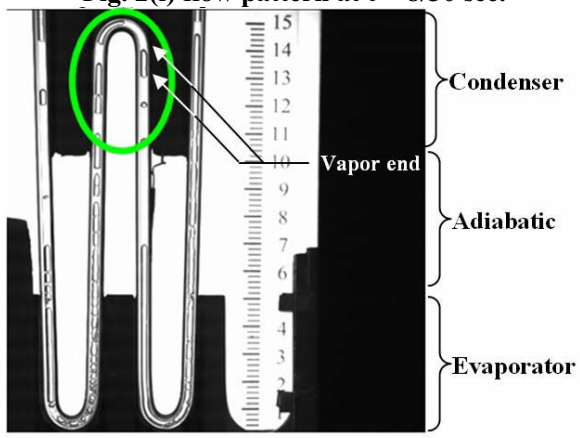


Fig. 2(j) flow pattern at t = 9/30 sec.

3.3 Heat transfer mechanism of CLOHP under assumption of constant operating pressure

The explanation of CLOHP heat transfer mechanism can be done by means of above assumption associate with consideration of figure 3. By marking with rectangle, figure 3(a) shows the vapor slug at the top of condenser section. Below the vapor slug, we can see the condensing liquid plug in the rectangle mark. Beneath the condensing liquid plug, there are groups of vapor slug along the tube to evaporator. In order to observe the circulate direction of working fluid, the ellipse marked vapor slug will be used as referent point. In the next time as shown in figure 3(b), the vapor at the top of rectangle condense and collapse from scale number 12 to number 14 while the liquid plug and the groups of vapor slug move upward to replace the collapse volume from scale number 11 to number 13. In this time, the referent vapor slug in ellipse mark has no displacement. We also can see vaporliquid junction, which be marked by a square, inside the evaporator section.

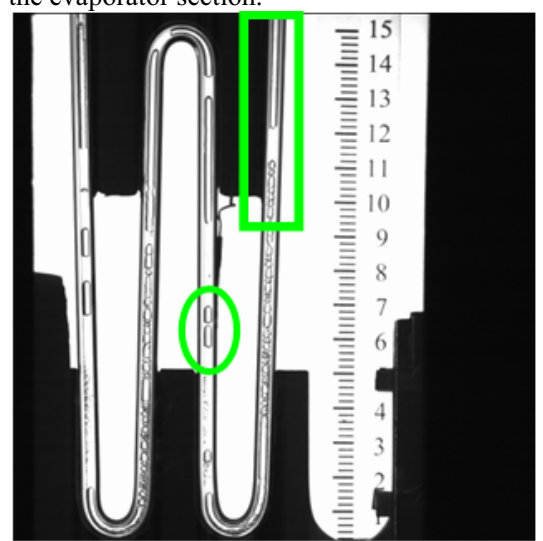


Fig. 3(a) flow pattern at initial observation

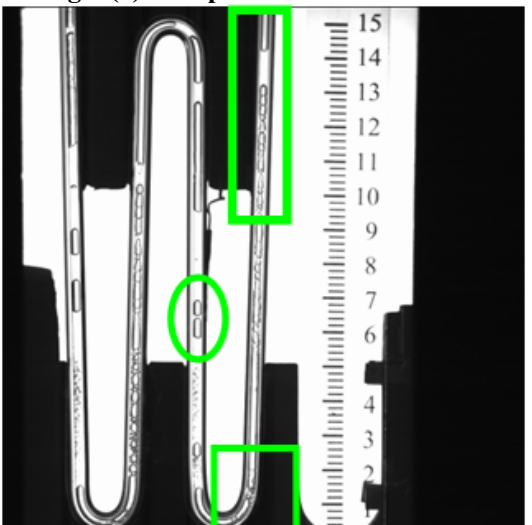


Fig. 3(b) flow pattern at t = 1/30 sec.

Next time step as shown in figure 3(c), the group of vapor slug move upward to the top of rectangle at scale number 15 while the referent vapor slug move

slightly downward to evaporator section from scale number 5.8 to 5.6. The vapor-liquid junction in a square mark moves upward higher than in fig 3(b) from scale number 1.4 to 2.8. The motion of vapor-liquid junction continuously occurs as shown in figure 3(d) and 3(e). Moreover, we can see the referent vapor slug slightly moves downward from scale number 5.7 to 5.4 while the vapor-liquid junction moves upward from scale number 4.6 to 5.8. When the junction already has left the evaporator section as shown in figure 3(e), liquid under the referent vapor slug will move downward to replace vacant volume in evaporator.

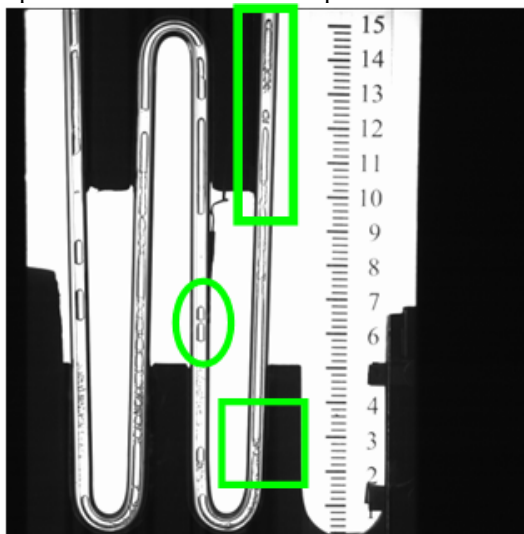


Fig. 3(c) flow pattern at t = 2/30 sec.

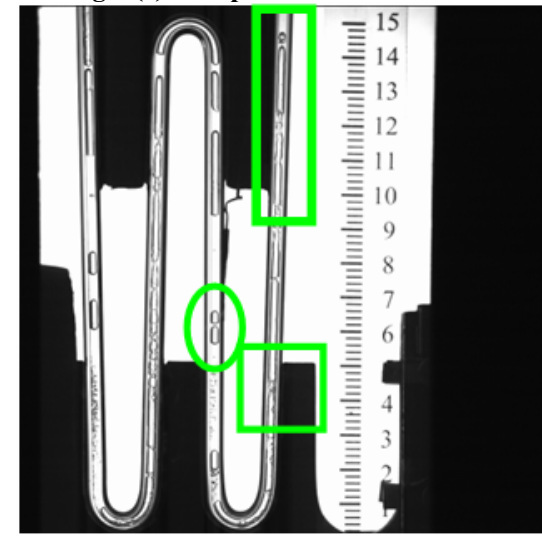


Fig. 3(d) flow pattern at t = 3/30 sec.

The referent vapor slug will also move downward into evaporator section from scale number 5.4 to 4.6. Now the replacement cycle is complete and there are liquid inside evaporator again as shown in figure 3(f). According to explanation above, the heat transfer mechanism of CLOHP can be described as follow, when liquid inside evaporator firstly receives heat from inner evaporator surface, the liquid will change to vapor phase in form of liquid-vapor slug train.

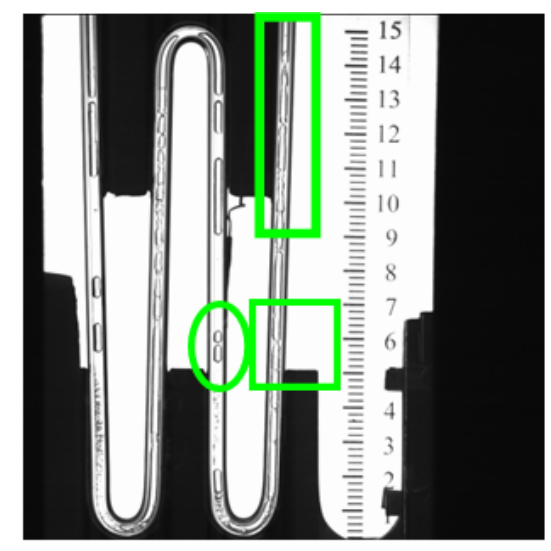


Fig. 3(e) flow pattern at t = 4/30 sec.

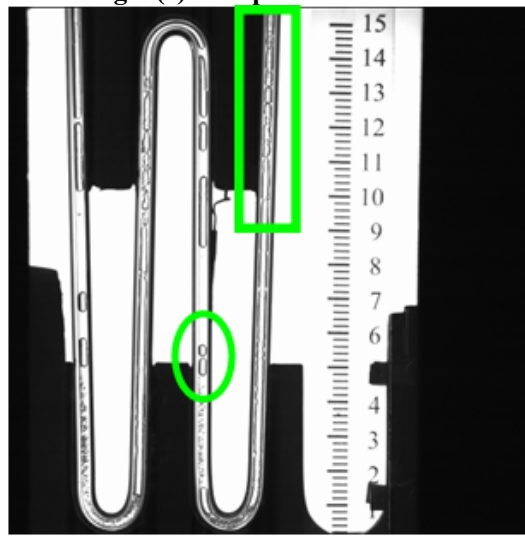
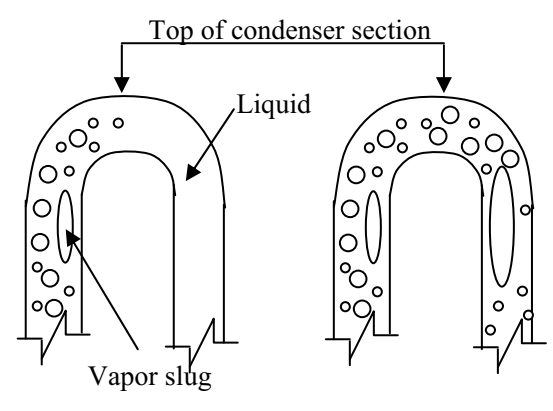


Fig. 3(f) flow pattern at t = 5/30 sec.

After that, the vapor slug in evaporator section will expand and push the adjacent mixture move in direction of replace the collapse volume in condenser as we can see in figure 3(a)-(b). This replacement will occur continuously. The returning liquid from condenser will replace the mixture which be pushed out from evaporator by vapor slug expansion as shown in figure 3(d)-(e). Thus, the replacement is a main driver of circulation in CLOHP. The replacement begins at condenser and finish at the evaporator. The important thing must be kept in mind is the expansion and collapse of vapor slug occur under the constant operating pressure. The circulation inside CLOHP is a result from replacement rather than from pressure difference.

In addition, the visual study data indicates that the circulation in CLOHP does not occur in a same direction all the time. In contrast, there is a change in direction of circulation inside CLOHP. This is because the incomplete condensation. Incomplete condensation is the event that vapor slug cannot condense to liquid without any vapor remaining before reach the top of condenser section. The incomplete condensation configuration is shown in figure 4



a. complete condensation b. Incomplete condensation

Fig. 4 incomplete condensation configuration

It is clear that the vapor in evaporator section will expand in direction which replace the condense volume in condenser section. Thus the rate of condensation at each side of condenser in a given turn is a flow direction controller of circulation. If condensation rate in each side of turn are equal, there is no direction of circulation in that turn. But if one side of turn has more condensation rate than the other one, the vapor in evaporator will expand in direction which more convenience i.e. the larger condensation rate side. The replacement process will occur and the circulation appears in direction forward from evaporator to the larger condensation rate side. However, effect of circulation will increase the vapor volume in a larger condensation rate side and results in rapidly decreasing of condensation rate on this side. This situation causes the incomplete condensation. The convenience direction for vapor expansion will change. The replacement process, consequently, will be unstable and the alternate direction of circulation will also occur. The above explanation is shown in figure 5 and 6

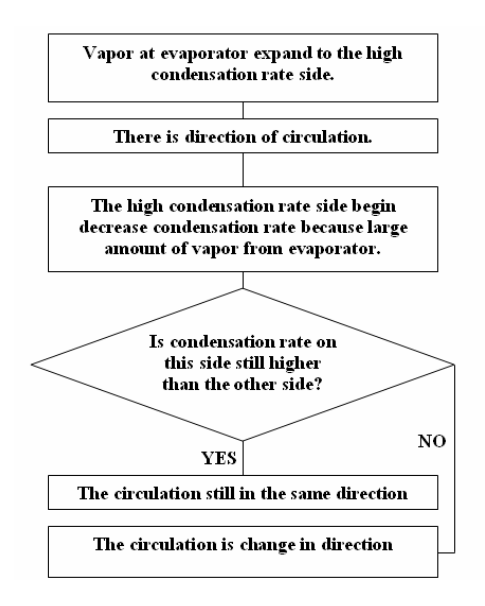


Fig. 5 shown the diagram of change in direction of circulation mechanism in CLOHP

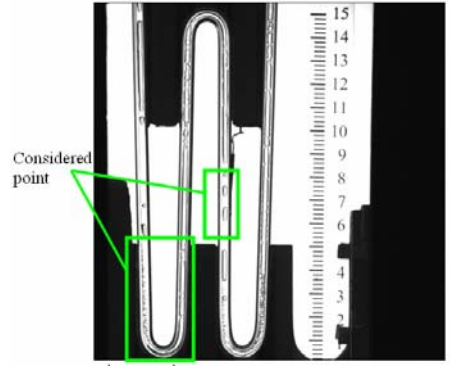


Fig. 6(a) shown the considered point in explanation of alternate direction of circulation

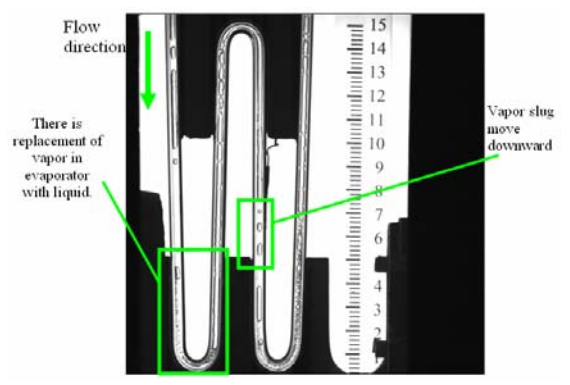


Fig. 6(b) shown the downward flow direction and replacement of vapor in evaporator section with liquid

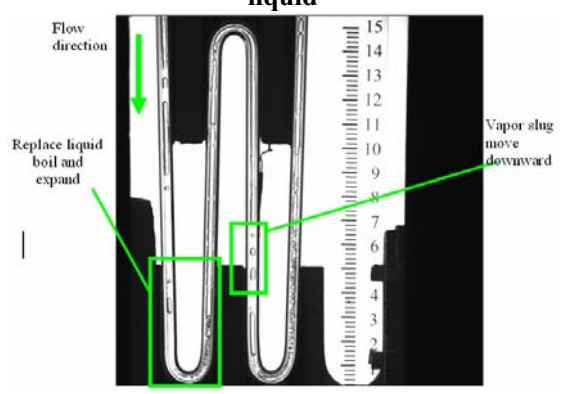


Fig. 6(c) shown the boiling and expansion of liquid in evaporator section

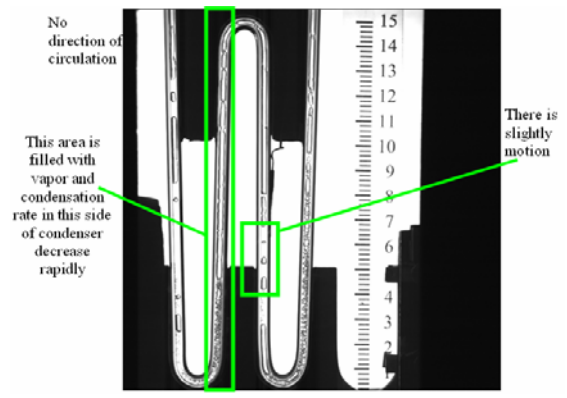


Fig. 6(d) shown the effect of incomplete condensation on the change in circulate direction

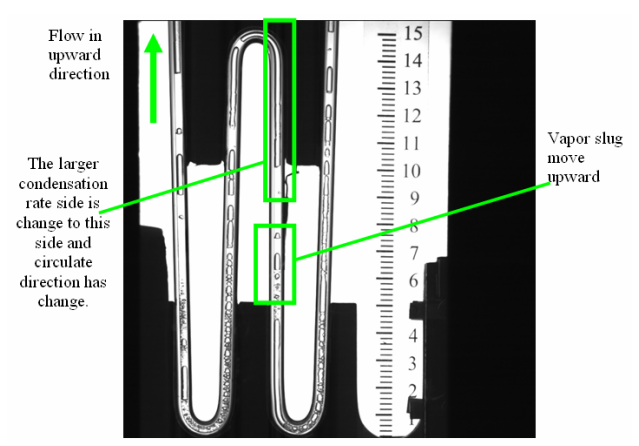


Fig. 6(e) shown the change in larger condensation rate side and circulate direction.
4. CONCLUSION

This paper shows the evidence from visual study to convince the new assumptions that vapor slug expand and collapse under constant operating pressure and quasi static condition. The expansion of vapor does not obey ideal gas law but due to the evaporation of liquid around the vapor slug. Moreover, the time series heat transfer mechanism of CLOHP will be explained. Finally the cause of alternate direction of circulation inside CLOHP will be clarified. These results lead to the new concept of CLOHP operation modeling and result in more understanding of CLOHP behavior and high accuracy prediction of CLOHP heat transfer rate.

Acknowledgements

All of this work cannot be conducted without the support from the Thailand Research Fund (Contract no. BRG4780024). The authors would also like to express their sincere appreciation.

References

- Charoensawan, P., Khandekar, S., Groll, M., and Terdtoon, P., Closed Loop Pulsating Heat Pipe Part A: Parametric Experimental Investigations. Applied Thermal Engineering. Vol. 23., 2003.
- Dobson, R.T., and Harms, T.M., Lumped Parameter Analysis of Closed and Open Oscillatory Heat Pipe. Procs. of the 11th International Heat Pipe Conference. Tokyo Japan., 1999.
- Khandekar, S., Charoensawan, P., Groll, M., and Terdtoon, P., Closed Loop Pulsating Heat Pipe Part B: Visualization and Semi-Empirical Modeling. Applied Thermal Engineering. Vol. 23., 2003.
- Lee, W., Jung, H., Kim, J., and Soo Kim, J., Characteristics of Pressure Oscillation in Selfexcited Oscillating Heat Pipe based on Experimental Study. Procs. of the 6th International Heat Pipe Symposium. Chiang Mai Thailand., 2000.
- Qu, W., and Ma, T., Experimental Investigation on Flow and Heat Transfer of a Pulsating Heat Pipe.
 Procs. of the 12th International Heat Pipe Conference. Russia., 2001.